

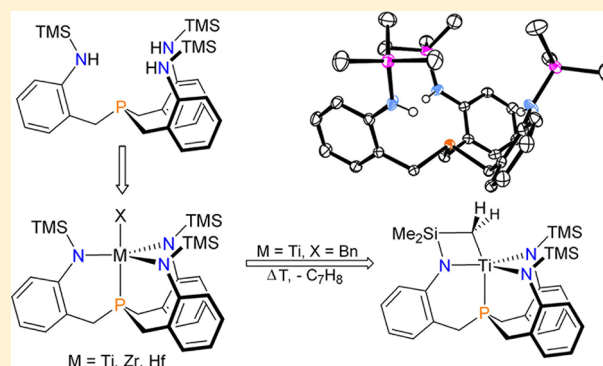
A Tripodal Benzylene-Linked Trisamidophosphine Ligand Scaffold: Synthesis and Coordination Chemistry with Group(IV) Metals

Sonja Batke, Malte Sietzen, Hubert Wadepohl, and Joachim Ballmann*

Anorganisch-Chemisches Institut, Universität Heidelberg, Im Neuenheimer Feld 276, 69120 Heidelberg, Germany

Supporting Information

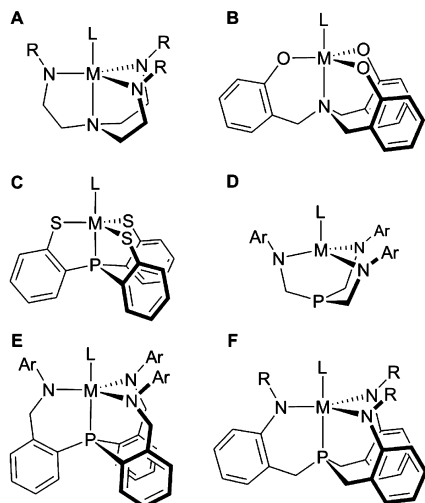
ABSTRACT: A new tripodal trisamidophosphine ligand (**1**) based on the trisbenzylphosphine backbone has been synthesized in three steps starting from NaPH_2 and phthaloyl-protected 2-aminobenzyl bromide. At elevated temperatures, **1** reacts directly with $\text{M}(\text{NMe}_2)_4$ ($\text{M} = \text{Zr}, \text{Hf}$) to afford the dimethylamido complexes $[\text{PN}_3]\text{M}(\text{NMe}_2)$ ($\text{M} = \text{Zr}, \text{Hf}$) (**2**), which are easily converted into the corresponding triflates $[\text{PN}_3]\text{MOTf}$ ($\text{M} = \text{Zr}, \text{Hf}$) (**3**) via reaction with triethylsilyl trifluoromethanesulfonate. The related titanium chloro complex $[\text{PN}_3]\text{TiCl}$ (**4-Ti**) is obtained from **1** and Bn_3TiCl via protonolysis. Triple deprotonation of **1** with *n*-butyllithium affords the tris-lithium salt $\text{Li}_3[\text{PN}_3]$ (**1-Li**), which serves as a common starting material for the preparation of all the group(IV) chlorides $[\text{PN}_3]\text{MCl}$ ($\text{M} = \text{Ti}, \text{Zr}, \text{Hf}$) (**4**). Upon treatment of **4-Ti** with $\text{Bn}_2\text{Mg}(\text{thf})_2$, formation of a benzyltitanium species is observed, which is converted cleanly into a ligand-CH-activated species (**5-Ti**).



INTRODUCTION

When Verkade and co-workers reported the first titanium complex that employs the *tren* framework as a tetradentate trisanion in 1991,¹ the term metallazatrane was coined to describe such inherently C_3 -symmetric complexes, which incorporate the *tren*-ligand in its trisanionic form. Soon after this seminal work, derivatives of the original N,N',N'' -trimethyl-*tren* system ($\text{A}, \text{R} = \text{Me}$, Chart 1) were developed by Verkade,² Schrock,³ and Gade,⁴ and it was shown that this privileged

Chart 1. Selection of C_3 -Symmetric Complexes That Employ Trisanionic Ligand Scaffolds

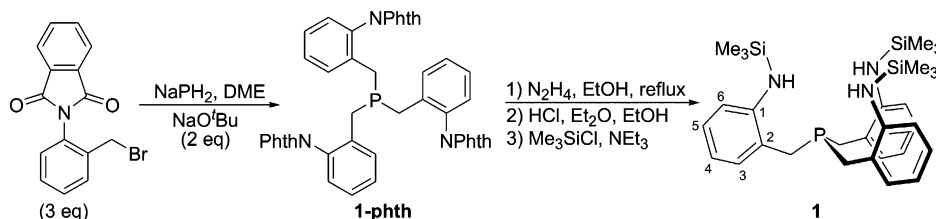


ligand scaffold coordinates to numerous transition metals⁵ and main block elements.⁶ Complexes of this type have found widespread applications in organic and inorganic chemistry, for example, in small molecule activation,⁷ dehydrocoupling reactions,⁸ polymerizations,⁹ or simply as an effective proton acceptor (Verkade's base¹⁰). Nowadays, over 50 derivatives of *tren* (commonly abbreviated with $[\text{NN}_3]$)¹¹ and related trisanionic ligand systems with $[\text{NO}_3]$,¹² $[\text{NS}_3]$,¹³ and $[\text{PS}_3]$ ¹⁴ donor sets are well-established (c.f. **B** and **C**, Chart 1). Surprisingly, trisanionic $[\text{PN}_3]$ -systems are rare, and so far, only the C_1 -linked ($\text{C}_1 = \text{methylene}$) system $\text{P}(\text{CH}_2\text{NHAr})_3$ has been used in coordination chemistry.¹⁵ In contrast to **A**, **B**, and **C**, this particular ligand scaffold coordinates in a tridentate fashion, leaving the phosphine *exo*-configured (**D**, Chart 1). In the context of dinitrogen activation, beneficial effects upon formal exchange of the central *tren*-nitrogen for a phosphine have been predicted on a theoretical basis,¹⁶ but these theoretical studies suppose a tetradentate coordination of a trisanionic $[\text{PN}_3]$ -ligand. Thus, efforts have been made to access coordination compounds of tris(2-aminoethyl)-phosphine (phospha-*tren*) and other potentially tetradentate trisamidophosphines. Although C_2 -linked $[\text{PN}_3]$ -ligands ($\text{C}_2 = \text{ethylene, phenylene}$) have been prepared,¹⁷ it seems that their complexes are not readily accessible, possibly due to formation of polymeric species.

Very recently, we demonstrated that the C_3 -linked trisamidophosphine ligand **E** (Chart 1) coordinates in a

Received: January 22, 2014

Published: April 8, 2014

Scheme 1. Ligand Synthesis (Arabic Numbers at **1** are Labels for NMR Signal Assignment)

tetradentate fashion upon ligation to group(IV) metals.¹⁸ As the latter system is based on a triphenylphosphine core, a limited donor strength of the apical phosphine (compared to phosphatren) had to be expected a priori. Nevertheless, the triatomic C₃-linkage in **E** proved to be appropriate for tetradentate binding to the central metal and inspired us to synthesize a [PN₃]-ligand with an inverted benzylene-spacer (i.e., a derivative of 2,2',2''-trisamino-trisbenzylphosphine, structure **F** in Chart 1) in order to establish the coordination chemistry of such a trisalkylphosphine-based [PN₃]-system. In this study, we focused on the tris-trimethylsilyl derivative of ligand **F** (R = SiMe₃), as silyl-aryl amines are commonly readily deprotonated even in cases of sterically demanding substituents.^{Sa,f-h,r} Compared to ligand **E** (containing three aryl-alkyl amines), a stabilizing effect has to be expected in complexes **F** (R = SiMe₃) due to the silyl substituents, which are located in β-positions with respect to the central metal.

RESULTS AND DISCUSSION

Ligand Synthesis. For the synthesis of an F-type ligand, three strategies were considered, namely, (i) metalation of *N*-protected *o*-toluidine at the benzylic position¹⁹ and subsequent reaction with a phosphorus electrophile (PCl₃, P(OPh)₃), (ii) synthesis of tris(*o*-nitrobenzyl)-phosphine and subsequent reduction, and (iii) synthesis of an *N*-protected primary *o*-aminobenzyl-phosphine²⁰ and subsequent reaction with the corresponding *N*-protected *o*-aminobenzyl bromide. In preliminary experiments, route (iii) was identified as the most promising approach as (*o*-phthalimido)-benzyl bromide²¹ reacts cleanly with primary phosphines. However, preparation of the key building block, (*o*-phthalimido)-benzyl-phosphine, proved to be more difficult than expected, although a potentially explosive procedure for the preparation of *o*-aminobenzyl-phosphine²⁰ was optimized successfully (see the Supporting Information). In an attempt to prepare (*o*-phthalimido)-benzyl-phosphine starting from (*o*-phthalimido)-benzyl bromide²¹ and NaPH₂,²² no primary phosphine, but a small amount of tris(*o*-phthalimidobenzyl)-phosphine, i.e., the phthaloyl-protected ligand scaffold (**1-Phth**), was isolated (Scheme 1). Treatment of NaPH₂ with 3 equiv of (*o*-phthalimido)-benzyl bromide in the presence of 2 equiv of sodium *tert*-butanolate in THF afforded **1-Phth** in low yields (approximately 10%). While changing to other alkali metal PH₂⁻ salts²³ or substitution of (*o*-phthalimido)-benzyl bromide for the respective chloride did not result in improved yields, the use of DME (DME = dimethoxyethane) instead of THF led to an enhanced procedure as the desired product forms in acceptable yields (approximately 30%) and precipitates straight from the reaction mixture along with sodium bromide (see Scheme 1). The inorganic salts are easily removed, and the key intermediate **1-Phth** thus obtained is sufficiently pure for subsequent deprotection. Employing a standard deprotection protocol via hydrazinolysis of the phthalimide,²⁴ the free amine was

generated and isolated in the form of its tris-hydrochloride salt. Starting from this salt, a trimethylsilyl substituent was attached to each of the three amino groups to obtain the desired ligand **1** as an off-white powder (Scheme 1).

As expected, **1** only exhibits one singlet in the ³¹P NMR spectrum at δ = -38.3 ppm, which is shifted upfield compared to Bn₃P (δ = -11.3 ppm²⁵) (Bn = benzyl). The ¹H NMR spectrum indicates that a highly symmetric species is present in solution, as only one set of signals is detected for the three individual side arms. Thus, one benzylic, one broadened NH, and one sharp trimethylsilyl signal are observed in addition to four aromatic resonances. Single crystals were grown by cooling a saturated solution of **1** in pentane to -40 °C and subjected to X-ray diffraction (see Figure 1), confirming the formation of

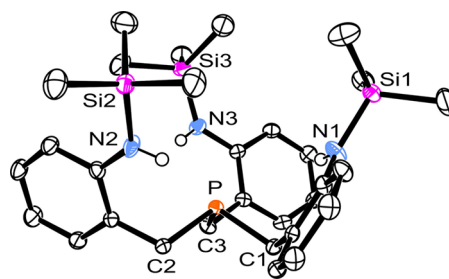
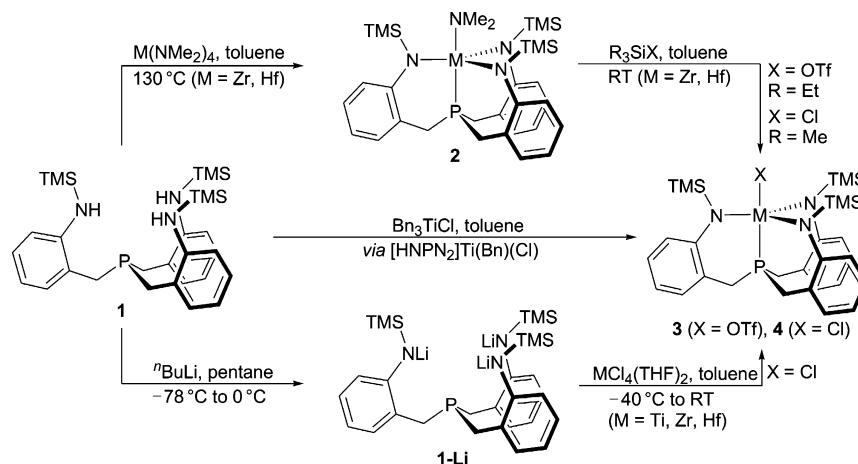


Figure 1. ORTEP plot of the molecular structure of **1** (carbon-bound protons omitted for clarity; thermal ellipsoids set at 50% probability). Selected bond lengths (Å) and angles (deg): Si1–N1 1.7376(14), Si2–N2 1.7306(13), Si3–N3 1.7428(14), P–C2 1.8532(14), P–C1 1.8542(15), P–C3 1.8576(14); C2–P–C1 99.66(7), C2–P–C3 101.13(7), C1–P–C3 101.46(7).

the target ligand. A particular interesting feature emerging from the molecular structure of **1** is that the ligand adopts a bowl-shaped conformation in the solid state, which appears to be ideally suited to host the targeted metal ions.

Complex Synthesis. Starting from **1**, the dimethylamido species [PN₃]M(NMe₂) **2** (M = Zr, Hf) were prepared by reaction with tetrakis(dimethylamido)zirconium and tetrakis(dimethylamido)hafnium, respectively (see Scheme 2). Prolonged heating (5 days in the case of Zr and 18 days in the case of Hf) at elevated temperatures (130 °C in toluene) is required to ensure full conversion, which favors the formation of several byproducts in addition to the target compounds. While the yield of crude products is in satisfactory ranges (approximately 65%), analytically pure material is only obtained in relatively modest yields (33% in the case of Zr and 35% in the case of Hf). According to ¹H and ¹³C NMR data, complexes **2** (M = Zr, Hf) are C₃-symmetric in solution, which implies free rotation of the dimethylamido substituent at room temperature. In the proton NMR spectra, diastereotopic resonances are observed for the methylene protons, indicating that the rotation of the three side arms along the 3-fold axis is hindered

Scheme 2. Synthesis of 1-Li, 2 (M = Zr, Hf), 3 (M = Zr, Hf), and 4 (M = Ti, Zr, Hf) Starting from 1



substantially. Even at 80 °C, no signs of a beginning coalescence of these signals are detectable, which renders the complexes configurationally stable. From a theoretical point of view, racemization in solution is possible via either a C_{3v} - or a C_5 -symmetric transition state (see the Supporting Information), but not observed experimentally for any of the compounds described herein (2-M to 4-M, M = Ti, Zr, Hf). The ^{31}P NMR spectra exhibit a single resonance at 17.2 ppm (2-Zr) and 26.7 ppm (2-Hf), respectively. While this rather unusual difference in ^{31}P NMR shifts (almost 10 ppm) is certainly noteworthy, we are unable to provide an explanation for this phenomenon, as the ^{31}P NMR resonances of all other zirconium and hafnium complexes in this work (vide infra) differ by less than 5.5 ppm (cf. 4-Zr and 4-Hf). If the apical phosphines in 2-Zr and 2-Hf are actually coordinated (*endo*-configuration) or pointing away from the central metals (*exo*-configuration) can be extracted neither from these ^{31}P NMR shifts nor from the ^1H or ^{13}C NMR data. To address this question, crystals of both the zirconium and the hafnium derivative of 2 were grown from saturated toluene solutions and examined by X-ray diffraction methods (see Figure 2 and Figure S2 in the Supporting Information). The structural analysis reveals both complexes to be *endo*-configured with metal–phosphorus bond distances well within the usual range²⁶ (2-Zr: Zr–P1 = 2.7284(13) Å; 2-Hf:

Hf–P = 2.7154(5) Å). All metrical parameters within the ligand framework display typical values, which is also the case for the distances between the amido nitrogens and the central metal ions. The coordination polyhedra in 2 deviate only slightly from ideally trigonal-bipyramidal structures (N1, N2, and N3 in equatorial positions) with an averaged $N_{\text{eq}}\text{--M--}N_{\text{eq}}$ angle of approximately 116° in both cases (M = Zr, Hf). The dimethylamido nitrogen atom N4 and the central phosphine of 2-Zr and 2-Hf are found in apical positions (P1–Zr–N4 = 173.55(4)°, P–Hf–N4 = 173.60(5)°) with the central metals located above the equatorial planes through N1, N2, and N3 (approximately 0.45 Å in 2-Zr and 0.43 Å in 2-Hf). Compared to 2-Zr (Zr–P1 = 2.7284(13) Å), the dimethylamido zirconium complex of ligand E (Chart 1, R = 3,5-xylyl; M = Zr; L = NMe₂) exhibits a metal–phosphorus distance of 2.824(1) Å.^{18a} This indicates a weaker interaction between the metal and the phosphine in the latter complex and demonstrates that the phosphine in ligand 1 is indeed a more electron-donating anchor (compared to the trisarylphosphine-based ligand E).

Complexes 2 are easily converted into the corresponding triflates 3 via reaction with triethylsilyl trifluoromethanesulfonate (see Scheme 2). Both triflates 3 (M = Zr, Hf) exhibit 3-fold symmetry in solution with only one singlet for the TMS groups (TMS = trimethylsilyl) present in the individual ^1H NMR spectra. Compared to the starting dimethylamido species 2, a downfield shift of the ^{31}P NMR resonances of 3 is observed and the product signals are detected at 26.3 ppm (3-Zr) and 29.6 ppm (3-Hf). For 3-Hf, single crystals suitable for X-ray diffraction were obtained by cooling a saturated toluene solution of the complex to –40 °C (see Figure 3). What is evident at a glance is that the central phosphine is still coordinated to the hafnium center and that the triflate occupies the remaining apical position of the trigonal-bipyramidal coordination polyhedron. Compared to 2-Hf, a significantly shorter Hf–P distance (2.647(2) and 2.654(2) Å in 3-Hf vs 2.7154(5) Å in 2-Hf) is noticed, while most other distances and angles within the [PN₃]Hf core differ only slightly or insignificantly. This stronger Hf–P interaction renders the phosphine more electropositive and explains the observed downfield shift in the ^{31}P NMR spectrum of 3-Hf (compared to 2-Hf). Compared to the corresponding hafnium triflate of ligand E (Chart 1, R = 3,5-xylyl; M = Zr; L = OTf), which displays a metal phosphorus distance of 2.713(1) Å, a shorter Hf–P distance is found for 3-Hf.^{18b} This effect is attributed to

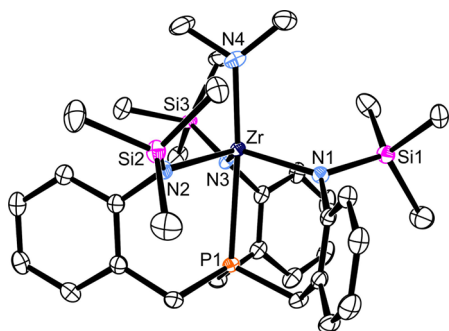


Figure 2. ORTEP plot of the molecular structure of 2-Zr (protons omitted for clarity; thermal ellipsoids set at 50% probability). Selected bond lengths (Å) and angles (deg): Zr–N4 2.0879(17), Zr–N1 2.0975(18), Zr–N2 2.1252(16), Zr–N3 2.1440(15), Zr–P1 2.7284(13); N4–Zr–N1 104.96(6), N4–Zr–N2 96.69(6), N1–Zr–N2 115.99(5), N4–Zr–N3 105.23(6), N1–Zr–N3 113.74(6), N2–Zr–N3 117.09(6), N4–Zr–P1 173.55(4), N1–Zr–P1 78.18(4), N2–Zr–P1 76.87(4), N3–Zr–P1 78.17(4).

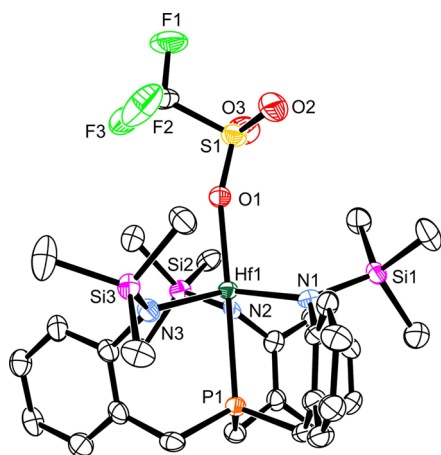


Figure 3. ORTEP plot of the molecular structure of 3-Hf (protons omitted for clarity; thermal ellipsoids set at 50% probability). In addition to the shown molecule, there is a second independent molecule with fairly similar metrical parameters present in the unit cell. Selected bond lengths (Å) and angles (deg) (values in square brackets refer to the second molecule): Hf1–P1 2.647(2) [2.654(2)], Hf1–O1 2.143(7) [2.144(7)], Hf1–N2 2.067(8) [2.085(9)], Hf1–N1 2.080(9) [2.082(8)], Hf1–N3 2.088(9) [2.074(9)]; O1–Hf1–P1 178.8(2) [178.5(2)], N2–Hf1–P1 79.8(2) [80.5(3)], N2–Hf1–O1 100.3(3) [99.7(3)], N2–Hf1–N1 114.6(3) [118.1(4)], N2–Hf1–N3 117.9(3) [115.9(4)], N1–Hf1–P1 80.2(2) [79.2(3)], N1–Hf1–O1 100.7(3) [99.5(3)], N1–Hf1–N3 118.4(4) [116.9(4)], N3–Hf1–P1 79.7(3) [80.0(2)], N3–Hf1–O1 99.2(3) [101.2(3)].

the different designs of ligands **E** and **1** and was expected a priori. Once attached to the metal, however, complexes of ligands **E** and **1** react in a rather similar way, which is noticed, for example, in the preparation of the $[\text{PN}_3]\text{MOTf}$ complexes ($M = \text{Zr}, \text{Hf}$, $[\text{PN}_3] = \text{ligand E, 1}$), as equivalent synthetic routes starting from the respective dimethylamido complexes are employed in both cases.¹⁸

Similar to the triflates **3**, the corresponding chlorides $[\text{PN}_3]\text{MCl}$ (**4-Zr** and **4-Hf**) are readily prepared by addition of trimethylsilyl chloride to solutions of **2** ($M = \text{Zr}, \text{Hf}$) in toluene (see Scheme 2). The proton NMR spectra of **3-Zr** and **4-Zr** exhibit only minor differences, and the ^{31}P NMR resonances are almost identical (26.3 ppm for **3-Zr** vs 26.2 ppm for **4-Zr**). For hafnium, the former differences are slightly more pronounced with ^{31}P NMR resonances found at 29.6 ppm for **3-Hf** and at 31.7 ppm for **4-Hf**, although **3** and **4** can be considered equivalent from a chemical point of view. Interestingly, zirconium and hafnium react almost identically when attached to the trisamidophosphine ligand **1**. This was also noticed in the preparation of **2** ($M = \text{Zr}, \text{Hf}$), as the reaction of $\text{M}(\text{NMe}_2)_4$ ($M = \text{Zr}, \text{Hf}$) with **1** occurs for zirconium as well as for hafnium employing rather similar reaction conditions. In contrast to its heavier homologues, a mixture of unidentified products was obtained upon reaction of **1** with tetrakis(dimethylamido)titanium. According to ^{31}P NMR spectroscopy, at least five species in approximately equal amounts had formed and no signal corresponding to a titanium-bound dimethylamido substituent was detected by ^1H NMR spectroscopy. Similarly, treatment of **1** with $(\text{Me}_2\text{N})_2\text{-TiCl}_2$ ²⁷/ LiNMe_2 or with $(\text{Me}_2\text{N})_3\text{-TiCl}$ ²⁸ failed to produce closed-cage complexes, but resulted in the formation of a species with one dangling side arm or in a trinuclear species ($[\text{HNPN}_2]\text{TiCl}_2$, $[(\text{TMS})_2\text{PN}_3]_2\text{Ti}_3$; see the Supporting Information). Reaction of **1** with Bn_4Ti ²⁹ also results in the

formation of unidentified mixtures. In contrast, treatment of **1** with Bn_3TiCl proceeds cleanly via the isolable intermediate $[\text{HNPN}_2]\text{Ti}(\text{Bn})(\text{Cl})$ (see the Supporting Information) and results in the formation of the desired $[\text{PN}_3]\text{TiCl}$ complex (**4-Ti**; see Scheme 2).

As the synthesis of **4** ($M = \text{Ti}, \text{Zr}, \text{Hf}$) suffered from the cumbersome preparation of Bn_3TiCl ²⁹ or from the time-consuming preparations of the required precursors **2** ($M = \text{Zr}, \text{Hf}$), an alternative synthetic pathway to the entire series **4** ($M = \text{Ti}, \text{Zr}, \text{Hf}$) was highly desirable. With the $\text{MCl}_4(\text{THF})_2$ precursors ($M = \text{Ti}, \text{Zr}, \text{Hf}$) readily available for all group(IV) metals,³⁰ the preparation of **4** via the tris-lithium salt $\text{Li}_3[\text{PN}_3]$ (**1-Li**) was explored. The required lithium salt **1-Li** was easily prepared in high yield (89%) by treatment of a cold solution of **1** in pentane with 3 equiv of *n*-butyl lithium and isolated as a THF adduct. According to ^1H NMR integration, 1 equiv of THF is present per cation, and all three lithium nuclei are equivalent according to ^7Li NMR ($\delta = 0.29$ ppm). The ^{31}P NMR spectrum of **1-Li** in $\text{THF-}d_6$ exhibits a singlet at -32.3 ppm, i.e., downfield shifted with respect to the protioligand **1** ($\delta = -38.3$ ppm). Thus, a weak coordinative interaction between the lithium and the phosphorus nuclei seems to be present at room temperature, although no coupling between the two nuclei was observed. Single crystals of **1-Li** suitable for X-ray diffraction were obtained from saturated $\text{Et}_2\text{O}/\text{THF}$ solutions and subjected to X-ray diffraction (see Figure 4). The molecular structure in the solid state does not reflect the structure present in solution, as one of the lithium ions is coordinated by solvent

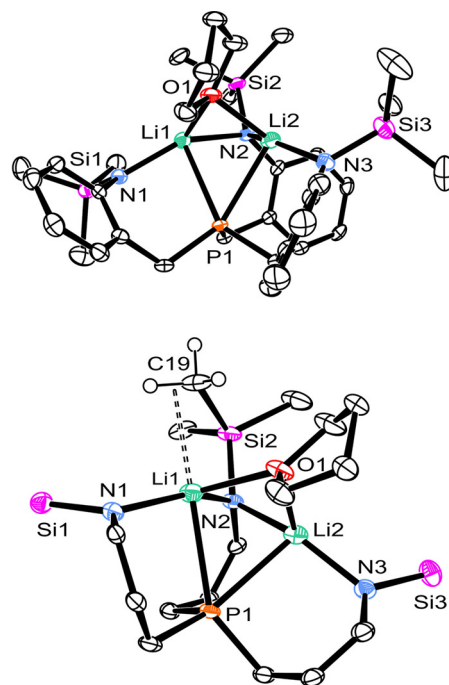


Figure 4. ORTEP plot of the molecular structure of the anion of **1-Li** (top) (hydrogen atoms and $\text{Li}(\text{OEt}_2)_2(\text{THF})_2$ counterion are omitted for clarity; thermal ellipsoids set at 50% probability) and detailed view of the core structure (bottom) (peripheral phenyl carbons, selected silylmethyl and hydrogen atoms omitted). Selected bond lengths (Å) and angles (deg): Li1...Li2 2.504(7), P1–Li1 2.602(5), P1–Li2 2.588(5), O1–Li1 2.240(6), O1–Li2 2.087(5), N1–Li1 1.969(6), N2–Li1 2.068(6), N2–Li2 2.138(6), N3–Li2 1.970(6); Li2–P1–Li1 57.69(16), Li2–O1–Li1 70.6(2), Li1–N2–Li2 73.1(2), O1–Li1–P1 91.87(19), O1–Li2–P1 95.9(2).

Table 1. Selected Metrical Parameters and ^{31}P NMR Shifts of **4** ($\text{M} = \text{Ti}, \text{Zr}, \text{Hf}$)

	4-Ti	4-Zr	4-Hf
M–P (Å)	2.5387(12)	2.6796(14)	2.6616(3)
M–N (Å)	1.9525(13)–1.9642(15)	2.0839(16)–2.0911(18)	2.0732(11)–2.0779(11)
M–Cl (Å)	2.3645(11)	2.4794(13)	2.4471(3)
P–M–Cl (deg)	173.119(17)	172.108(17)	172.909(11)
δ ^{31}P (ppm) ^a	40.7	26.2	31.7

^aRecorded in toluene- d_8 at room temperature.

molecules only (two THF and two Et_2O molecules). The latter lithium solvate serves as counterion for a monoanionic $[\text{PN}_3]\text{Li}_2(\mu\text{-THF})$ arrangement with two lithium ions located within the ligand's half-cage framework. In consequence, two ^7Li NMR signals in a 2 to 1 ratio are to be expected if this structure was also present in solution. Upon dissolution of the crystals in THF- d_8 , only the above-mentioned singlet was detected in the ^7Li NMR (**1-Li** is almost insoluble in C_6D_6 or toluene- d_8 and decomposes immediately in DMSO- d_6 or CD_2Cl_2 ; therefore, THF- d_8 is required for NMR spectroscopic studies). At -80 °C, all NMR signals (^1H NMR and $^{31}\text{P}\{^1\text{H}\}$ NMR) are broadened significantly or completely absent, which precludes a meaningful analysis. This is also the case if crystalline $[\text{Li}(\text{THF})_2(\text{OEt}_2)_2]\{[\text{PN}_3]\text{Li}_2(\mu\text{-THF})\}$ is dissolved in precooled THF- d_8 (-80 °C) and the NMR spectra recorded at -80 °C (precooled spectrometer). In the ^7Li NMR spectrum, a sharp peak (tentatively assigned to the solvated lithium cation) is observed at low temperatures in addition to unresolved broad signals (see the Supporting Information). Unfortunately, the observed ^7Li NMR shift for **1-Li** does not allow for a conclusive statement on coordination numbers or geometries, as ^7Li NMR signals of related lithium amides are found within -1.8 and $+4.9$ ppm (see the Supporting Information). On the basis of these observations, we propose that a dynamic exchange process sets in upon dissolution of **1-Li** in THF- d_8 and that this process renders all lithium atoms equivalent at room temperature.

Although unexpected at first, the molecular structure of **1-Li** in the solid state exhibits several interesting features (see Figure 4). Each of the lithium ions situated within the ligand's half-cage is bound to one individual amido side arm, and both metals are bridged by the remaining third amido side arm, by the phosphine, and by a THF molecule. In addition, an agostic interaction between Li1 and one of the silylmethyl groups seems to be present, as indicated by one unusual H–C19–H angle of approximately 95° and a short distance between the center of the respective C–H bond and Li1 (approximately 2.68 Å). Thus, the coordination geometry around Li1 is best described as distorted trigonal-bipyramidal with P1 and C19–H in axial positions and N1, N2, and O1 in the equatorial plane. For Li2, a distorted tetrahedral coordination environment is found. Particularly noteworthy is a relatively short intermetallic distance of 2.504(7) Å within the triply bridged bimetallic assembly.³¹

With **1-Li** in hand, the $[\text{PN}_3]\text{M}$ chlorides **4** ($\text{M} = \text{Ti}, \text{Zr}, \text{Hf}$) were generated by addition of a precooled suspension of **1-Li** in toluene to a suspension of $\text{MCl}_4(\text{thf})_2$ in toluene at -40 °C, and the respective products were isolated after the reaction mixtures had been warmed to room temperature over the course of 4–6 h. For zirconium and hafnium, this procedure led to the desired compounds **4-Zr** and **4-Hf** in high purity and acceptable yields (approximately 50%). For titanium, however, side-products formed in addition to the target material and had

to be removed by filtration over rigorously dried aluminum oxide. This rather unusual purification methodology works on small scales only, as prolonged contact with the aluminum oxide induces degradation of the complex. Despite numerous efforts to optimize this procedure, yields of pure **4-Ti** were consistently in the range of 20% only. Nevertheless, this procedure is preferred over the reaction of **1** with Bn_3TiCl (vide supra). Complex **4-Ti** is also generated by reaction of **1-Li** with $\text{TiCl}_3(\text{thf})_3$ and in situ oxidation with PbCl_2 . Unidentified impurities (approx 15% by ^{31}P NMR spectroscopy), however, could not be removed efficiently, which renders this procedure inapplicable.

Proton NMR spectra of all three complexes **4** indicate that the complexes are C_3 -symmetric in solution with only one resonance each observed for the equivalent sets of atoms of the individual side arms. A singlet in the ^{31}P NMR spectrum is detected for each complex, and an increasing shift to more positive δ values in the order **4-Zr** ($\delta = 26.2$ ppm) > **4-Hf** ($\delta = 31.7$ ppm) > **4-Ti** ($\delta = 40.7$ ppm) is noticed (see Table 1). As the ionic radii of the group(IV) metals decrease in the above order, the Lewis acidities increase in just the same way, if oxidation states and coordination numbers remain constant. Thus, the above trend of the ^{31}P NMR shifts might be explained by an increasingly stronger interaction between the metal and the phosphine donor provoked by an increasing Lewis acidity of the metal ion, as stronger M–P interactions lead to a deshielding of the ^{31}P nucleus. To substantiate this simple explanation, single crystals of **4** ($\text{M} = \text{Ti}, \text{Zr}, \text{Hf}$) for X-ray diffraction analysis were required in order to determine the metal phosphorus distances and to ensure that coordination numbers and other metrical parameters are within comparable boundaries. Fortunately, single crystals of all three complexes were obtained readily via diffusion of pentane into saturated solutions of the complexes in toluene (see Figure 5). Trigonal-bipyramidal coordination polyhedra with the amido donors occupying equatorial positions are found for all type-**4** complexes. The chlorides and phosphines are located in axial positions, and a similar deviation from linearity is observed for the individual P–M–Cl vectors (see Table 1). Comparison of the metal phosphorus distances in **4** ($\text{M} = \text{Ti}, \text{Zr}, \text{Hf}$) confirms the expected trend as the respective bond lengths decrease in the order of $\text{Zr–P} > \text{Hf–P} > \text{Ti–P}$.

With all chloro complexes **4** available, we turned the focus to the preparation of $[\text{PN}_3]\text{M}(\text{alkyl})$ species ($\text{M} = \text{Ti}, \text{Zr}, \text{Hf}$) and examined the reactions of **4** with Grignard reagents and dialkylmagnesium species, such as $\text{Bn}_2\text{Mg}(\text{THF})_2$.³² To our surprise, **4-Zr** and **4-Hf** do not react with different magnesium alkyls (MeMgBr , $\text{Me}_2\text{Mg}(\text{THF})_2$, PhMgBr , BnMgCl , $\text{Bn}_2\text{Mg}(\text{THF})_2$) not even after prolonged reaction times (up to 2 weeks) at elevated temperatures (90 °C). In contrast, **4-Ti** reacts slowly with $\text{Bn}_2\text{Mg}(\text{THF})_2$, and a new ^{31}P NMR signal appears at $\delta = -31.4$ ppm after several days at room temperature. However, incomplete conversion was observed

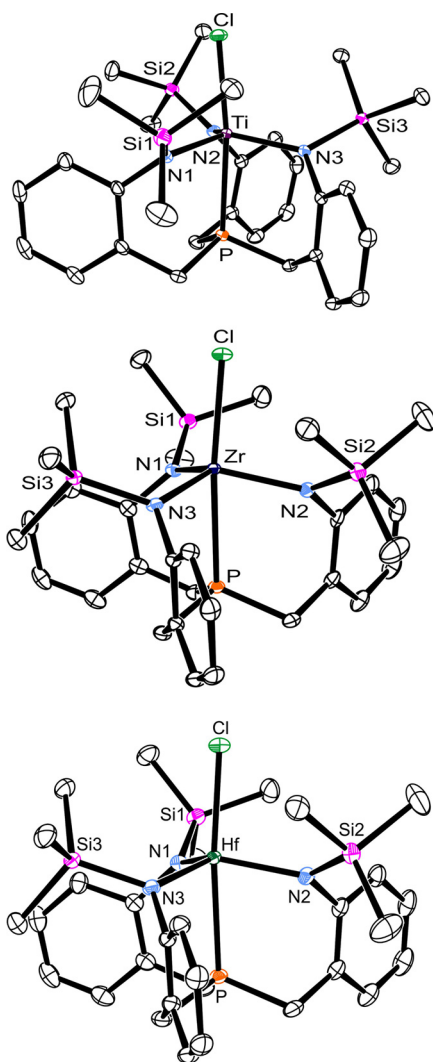


Figure 5. ORTEP plots of the molecular structures of **4-Ti** (top), **4-Zr** (middle), and **4-Hf** (bottom) (protons omitted for clarity; thermal ellipsoids set at 50% probability). Selected bond lengths (Å) and angles (deg) of **4-Ti**: Ti–Cl 2.3645(11), Ti–P 2.5387(12), Ti–N1 1.9525(13), Ti–N2 1.9642(15), Ti–N3 1.9559(14); Cl–Ti–P 173.119(17), N1–Ti–Cl 95.90(4), N1–Ti–P 79.86(4), N1–Ti–N2 122.03(6), N1–Ti–N3 116.66(6), N2–Ti–Cl 96.41(4), N2–Ti–P 81.47(4), N3–Ti–Cl 103.98(4), N3–Ti–P 82.82(4), N3–Ti–N2 114.62(5). Selected bond lengths (Å) and angles (deg) of **4-Zr**: Zr–Cl 2.4794(13), Zr–P 2.6796(14), Zr–N1 2.0911(18), Zr–N2 2.0839(16), Zr–N3 2.0891(17); Cl–Zr–P 172.108(17), N1–Zr–Cl 98.76(4), N1–Zr–P 78.78(4), N2–Zr–Cl 97.85(5), N2–Zr–P 77.13(5), N2–Zr–N1 119.05(7), N2–Zr–N3 116.26(6), N3–Zr–Cl 107.93(4), N3–Zr–P 79.87(4), N3–Zr–N1 113.18(6). Selected bond lengths (Å) and angles (deg) of **4-Hf**: Hf–Cl 2.4471(3), Hf–P 2.6616(3), Hf–N1 2.0779(11), Hf–N2 2.0732(11), Hf–N3 2.0777(11); Cl–Hf–P 172.909(11), N1–Hf–Cl 98.24(3), N1–Hf–P 79.53(3), N2–Hf–Cl 97.54(3), N2–Hf–P 77.99(3), N2–Hf–N1 119.74(4), N2–Hf–N3 116.62(4), N3–Hf–Cl 106.35(3), N3–Hf–P 80.66(3), N3–Hf–N1 113.64(4).

even in the case of an excess of $\text{Bn}_2\text{Mg}(\text{THF})_2$. On the basis of ^1H NMR analysis, the new species at $\delta(^{31}\text{P}) = -31.4$ ppm is tentatively assigned to $[\text{PN}_3]\text{TiBn}$. Upon heating a mixture of unreacted **4-Ti**, $\text{Bn}_2\text{Mg}(\text{THF})_2$, and $[\text{PN}_3]\text{TiBn}$, complete conversion to a new species at $\delta(^{31}\text{P}) = 24.3$ ppm was observed, and the resulting product **5-Ti** was isolated in 66% yield after work-up. What emerges from the ^1H NMR spectrum of **5-Ti** is

that the 3-fold symmetry is lost and that a compound with different side arms had formed. Six methylene protons of the ligands' benzyl moieties are observed along with overall 12 partially overlapping aryl signals. In addition to two singlets for the TMS groups, which integrate to 18 protons, two other methylsilyl resonances are detected at $\delta = 0.77$ ppm and $\delta = 0.00$ ppm with an intensity of three protons each. No signals for a titanium-bound benzyl ligand are detected, but two coupled doublets corresponding to one proton each are present at 2.38 and 1.21 ppm, respectively.

On the basis of this analysis, formation of a CH-activated species as shown in Scheme 3 is proposed. This is corroborated by ^{13}C , ^{13}C -DEPT, ^1H , ^{13}C -HSQC, ^1H , ^{13}C -HMBC, ^1H , ^1H -COSY, ^1H , ^{31}P -HMBC, and ^{29}Si NMR spectra, all of which are in agreement with the anticipated structure of **5-Ti**. As all attempts to crystallize **5-Ti** for single-crystal X-ray diffraction failed, the acquired NMR data were also compared to related systems known in literature. With trimethylsilyl substituted *tren*-ligands for example, two group(IV) azatranes that show a similar type of intraligand CH activation have been reported, namely, the $^{\text{TMS}}[\text{NN}_3]$ -titanium^{3b,c} and $^{\text{TMS}}[\text{NN}_3]$ -zirconium^{5b,33} derivatives. In both cases, similar proton NMR data, especially with respect to the metal-bound methylene group, are well-documented, thus supporting our structural assignment of **5-Ti** (see Scheme 3). In this context, it is noteworthy that the titanium–methyl complex of ligand E (see Chart 1) is prone to intraligand CH activation as well, while the corresponding zirconium and hafnium complexes do not show such reactivity.¹⁸ Thus, the titanium derivatives of the $[\text{PN}_3]$ -ligands E and F are directly comparable, while surprising differences in the initial complexation of titanium are apparent. With both ligands in hand, we will now continue to explore their (possibly dissimilar) coordination chemistry with other early transition metals and also focus on the reactivity of the CH-activated titanium complexes. While attempts to hydrogenate **5-Ti** were not productive yet, efforts to react **5-Ti**, for example, with silanes are ongoing in our laboratories and directed toward the application of this system as “hydride surrogate”.³⁴

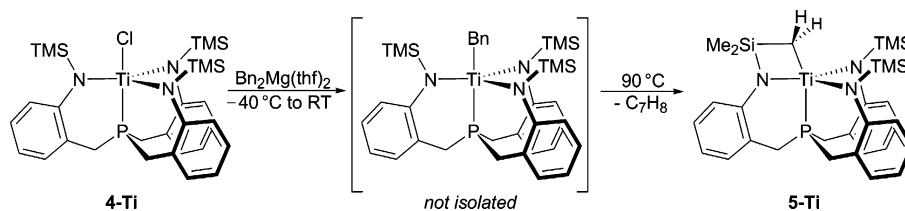
CONCLUSION

In conclusion, the new trisamidophosphine ligand **1** was synthesized and comprehensively characterized, and its coordination chemistry was examined with all of the group(IV) metals. For zirconium and hafnium, the dimethylamido and triflate species **2** and **3** were prepared and their structures were elucidated by X-ray crystallography. A synthetic pathway that affords the $[\text{PN}_3]\text{MCl}$ (**4**, $\text{M} = \text{Ti}, \text{Zr}, \text{Hf}$) species via the lithium salt **1-Li** was developed, and all complexes **4** and the lithium salt **1-Li** were studied in detail. Reaction of $\text{Bn}_2\text{Mg}(\text{THF})_2$ with **4-Ti** results in a ligand-CH-activated species (**5-Ti**) and provides a basis for further studies employing **5-Ti**, for example, in dehydrocoupling reactions.³⁴

EXPERIMENTAL SECTION

General Methods. All manipulations were performed under an atmosphere of dry and oxygen-free argon by means of standard Schlenk or glovebox techniques. Solvents were either taken from an M. Braun Solvent Purification System (THF, Et_2O , toluene, *n*-hexane, and *n*-pentane) or dried over CaH_2 and distilled (TMS_2O , CH_2Cl_2) (TMS_2O = hexamethyldisiloxane). Toluene- d_6 , THF- d_6 , and benzene- d_6 were refluxed over sodium and purified by distillation. NEt_3 was dried over CaH_2 and purified by distillation. DME was dried over

Scheme 3. Synthesis of 5-Ti Starting from 4-Ti



sodium benzophenone ketyl and EtOH over magnesium tunings, and both were purified by distillation. Hydrazine monohydrate was degassed by three freeze–pump–thaw cycles and kept under an atmosphere of dry argon. Triethylsilyl trifluoromethanesulfonate and trimethylsilyl chloride were purified by simple distillation prior to use. ^{31}P , ^1H , and ^{13}C NMR spectra were recorded on a Bruker Avance 600 MHz or a Bruker Avance 400 MHz spectrometer at room temperature. ^1H and ^{13}C NMR spectra were referenced to residual proton signals of the lock solvents. ^{31}P NMR spectra were referenced to external $\text{P}(\text{OMe})_3$ (141.0 ppm with respect to 85% H_3PO_4 at 0.0 ppm). Assignments of the NMR signals (see Scheme 1 for atom numbering) and coupling constants ($J_{\text{H,P}}$ vs $J_{\text{H,H}}$) were ascertained by ^1H , ^1H –COSY, ^{13}C –DEPT, ^1H , ^{13}C –HSQC, ^1H , ^{13}C –HMBC, and $^1\text{H}\{^{31}\text{P}\}$ NMR spectroscopy. Microanalyses (C, H, N) were performed at the Department of Chemistry at the University of Heidelberg. Especially in the case of the zirconium and hafnium complexes, severe difficulties were encountered in obtaining satisfactory elemental analyses. As carbon values were found reproducibly too low, it is assumed that carbides of the metals form during combustion. This hypothesis is supported by the fact that almost all elemental analyses are satisfactory, if a stoichiometric amount of carbon is deducted from the theoretical carbon value. However, unambiguous proof for this assumption cannot be provided; therefore, theoretical values are given without subtraction of a carbon atom. The starting materials (*o*-phthalimido)-benzyl bromide, 21 NaPH_2 , 22a Bn_3TiCl , 29 $\text{MCl}_4(\text{THF})_2$ ($\text{M} = \text{Ti}, \text{Zr}, \text{Hf}$), 30 and $\text{Bn}_2\text{Mg}(\text{thf})_2$ 32 were synthesized according to published procedures. The dimethylamido precursors $\text{M}(\text{NMe}_2)_4$ ($\text{M} = \text{Ti}, \text{Zr}, \text{Hf}$), *n*-butyl lithium solutions (2.5 M in hexanes), sodium *tert*-butanolate, and hydrogen chloride solutions (2.0 M in Et_2O) were purchased from Aldrich and used as received.

(phth) $_3$ [PN $_3$] (1-Phth). To a stirred suspension of NaPH_2 (0.78 g, 14 mmol, 1.0 equiv) and NaO^tBu (2.24 g, 28 mmol, 2.0 equiv) in DME (50 mL) was added solid (*o*-phthalimido)-benzyl bromide (13.3 g, 42 mmol, 3.0 equiv) in portions over a period of 20 min, and the resulting mixture was stirred for 7 h at room temperature. The crude product precipitated over the course of the reaction and was filtered off subsequently. The obtained pale yellow solid was washed with DME (2 \times 10 mL) and dried in vacuum. Residual NaBr was removed by washing the crude material with deoxygenated water (3 \times 30 mL) to afford the product as a colorless solid (8.5 g, 11.4 mmol, 82%) (phth = phthaloyl). ^1H NMR (600 MHz, $\text{DMSO}-d_6$): δ [ppm] = 8.01–7.93 (m, Phth-ArH, 6 H), 7.89–7.81 (m, Phth-ArH, 6 H), 7.22 (d, $^3J_{\text{H,H}} = 7.6$ Hz, 5-ArH, 3 H), 7.19 (t, $^3J_{\text{H,H}} = 7.4$ Hz, 6-ArH, 3 H), 7.07 (d, $^3J_{\text{H,H}} = 7.6$ Hz, 3-ArH, 3 H), 7.03 (t, $^3J_{\text{H,H}} = 7.4$ Hz, 4-ArH, 3 H), 2.54 (s, PCH_2 , 6 H). ^{13}C NMR (151 MHz, $\text{DMSO}-d_6$): δ [ppm] = 167.4 (s, NCO), 137.3 (d, $^3J_{\text{C,P}} = 6.8$ Hz, 1-ArC), 134.9 (s, Phth-ArC), 132.2 (s, 3-ArCH), 131.2 (d, $^2J_{\text{C,P}} = 3.7$ Hz, 2-ArC), 130.1 (d, $^4J_{\text{C,P}} = 0.9$ Hz, 6-ArCH), 129.2 (s, 4-ArCH), 127.1 (s, 5-ArCH), 124.1 (s, Phth-ArCH), 123.9 (s, Phth-ArCH), 30.0 (d, $^1J_{\text{C,P}} = 18.6$ Hz, PCH_2). $^{31}\text{P}\{^1\text{H}\}$ NMR (162 MHz, $\text{DMSO}-d_6$): δ [ppm] = –15.6 (s). MS (FAB+): m/z (%) = 762.2 [$\text{M} + \text{Na}$] $^+$ (100%). M ($\text{C}_{45}\text{H}_{30}\text{N}_3\text{O}_6\text{P}$) = 739.71 g mol^{-1} . HRMS (FAB+): calcd. for $\text{C}_{45}\text{H}_{30}\text{N}_3\text{NaO}_6\text{P}$: 762.1770, found 762.1748.

$\text{H}_3[\text{PN}_3]$ (1). To a suspension of 1-Phth (8.30 g, 11.2 mmol, 1.0 equiv) in ethanol (150 mL) was added hydrazine monohydrate (1.85 g, 37.1 mmol, 3.2 equiv) dropwise, and the resulting reaction mixture was refluxed for 2 h. After cooling to room temperature, a solution of hydrogen chloride in Et_2O (2.0 M, 37 mL, 74.2 mmol, 6.6 equiv) was added and the mixture was refluxed for an additional hour. Diethyl

ether and excess hydrogen chloride were then removed under reduced pressure, and the suspension was cooled to 0 $^\circ\text{C}$. Insoluble phthaloylhydrazide was filtered off, and the filtrate was condensed to dryness. The residual solid was suspended in methylene chloride (200 mL), and triethylamine (11.5 mL, 85 mmol, 7.6 equiv) was added subsequently. The reaction mixture was stirred for 20 min at room temperature, and trimethylsilyl chloride (21.7 mL, 170 mmol, 15.2 equiv) was added dropwise over a period of 15 min. Stirring was continued for 16 h at room temperature, and all volatiles were then removed in vacuum. The resulting white residue was extracted with pentane (3 \times 50 mL), and the filtrate was condensed to dryness. The residual crude product was triturated with TMS_2O , and the insoluble product was isolated via filtration. After removal of residual TMS_2O in vacuum, the product was obtained as an off-white solid (1.89 g, 3.35 mmol, 29%). ^1H NMR (600 MHz, C_6D_6): δ [ppm] = 7.12–7.06 (m, 5-ArH, 3 H), 6.94 (d, $^3J_{\text{H,H}} = 7.4$ Hz, 3-ArH, 3 H), 6.86 (d, $^3J_{\text{H,H}} = 8.0$ Hz, 6-ArH, 3 H), 6.75 (t, $^3J_{\text{H,H}} = 7.4$ Hz, 4-ArH, 3 H), 3.34 (s, NH, 3 H), 2.58 (s, PCH_2 , 6 H), 0.08 (s, SiMe_3 , 27 H). ^{13}C NMR (151 MHz, C_6D_6): δ [ppm] = 145.5 (d, $^3J_{\text{C,P}} = 3.4$ Hz, 1-ArC), 131.0 (d, $^3J_{\text{C,P}} = 5.2$ Hz, 3-ArCH), 128.4 (s, 5-ArCH), 124.2 (d, $^2J_{\text{C,P}} = 5.3$ Hz, 2-ArC), 118.4 (d, $^4J_{\text{C,P}} = 2.3$ Hz, 4-ArCH), 117.0 (d, $^4J_{\text{C,P}} = 1.6$ Hz, 6-ArCH), 32.4 (d, $^1J_{\text{C,P}} = 17.4$ Hz, PCH_2), 0.10 (s, SiMe_3). $^{31}\text{P}\{^1\text{H}\}$ NMR (243 MHz, C_6D_6): δ [ppm] = –38.3 (s). MS (FAB+): m/z (%) = 566.3 [$\text{M} + \text{H}$] $^+$ (100%). HRMS (FAB+): calcd. for $\text{C}_{30}\text{H}_{48}\text{N}_3\text{PSi}_3$: 565.2894, found 565.2992. M ($\text{C}_{30}\text{H}_{48}\text{N}_3\text{PSi}_3$) = 565.95 g mol^{-1} . Elemental analysis calcd. for $\text{C}_{30}\text{H}_{48}\text{N}_3\text{PSi}_3$: C 63.29, H 8.35, N 5.27; found: C 62.80, H 8.91, N 4.73.

$\text{Li}_3[\text{PN}_3](\text{thf})_3$ (1-Li). THF (1.00 mL, 800 mg, 11.0 mmol, 12 equiv) was added to a suspension of 1 (500 mg, 885 μmol , 1.0 equiv) in pentane (20 mL), and the mixture was stirred at room temperature until all solids dissolved (5–10 min). The resulting solution was cooled to –78 $^\circ\text{C}$, and *n*-BuLi (2.5 M in hexane, 1.11 mL, 2.77 mmol, 3.14 equiv) was added dropwise within 10 min. The solution was stirred for 30 min at –78 $^\circ\text{C}$ and brought to 0 $^\circ\text{C}$. After stirring for 90 min at 0 $^\circ\text{C}$, the reaction mixture was filtered at this temperature and washed with cold pentane (3 \times 10 mL). The remaining solids were dried in vacuum, and the product was obtained as a beige powder (628 mg, 786 μmol , 89%). ^1H NMR (600 MHz, $\text{THF}-d_8$): δ [ppm] = 6.71 (d, $^3J_{\text{H,H}} = 6.8$ Hz, 6-ArH, 3 H), 6.56 (t, $^3J_{\text{H,H}} = 7.8$ Hz, 4-ArH, 3 H), 6.49 (d, $^3J_{\text{H,H}} = 7.8$ Hz, 3-ArH, 3 H), 6.02 (t, $^3J_{\text{H,H}} = 7.0$ Hz, 5-ArH, 3 H), 3.61 (s, THF, 12 H), 2.91 (s, PCH_2 , 6 H), 1.77 (s, THF, 12 H), –0.07 (s, SiMe_3 , 27 H). ^{13}C NMR (101 MHz, $\text{THF}-d_8$): δ [ppm] = 160.7 (s, 1-ArC), 131.0 (s, 2-ArC), 129.2 (d, $^4J_{\text{C,P}} = 4.9$ Hz, 6-ArCH), 124.9 (s, 4-ArCH), 123.2 (s, 3-ArCH), 110.9 (s, 5-ArCH), 33.0 (s, PCH_2), 2.7 (s, SiMe_3). $^{31}\text{P}\{^1\text{H}\}$ NMR (243 MHz, $\text{THF}-d_8$): δ [ppm] = –32.3 (s). ^7Li NMR (155 MHz, $\text{THF}-d_8$): δ [ppm] = 0.29 (s). MS (ESI+): m/z (%) = 578.3 [$\text{M} - 3\text{THF} - \text{Li} + 2\text{H}$] $^+$ (100%). M ($\text{C}_{30}\text{H}_{45}\text{Li}_3\text{N}_3\text{PSi}_3 \times 3\text{THF}$) = 800.07 g mol^{-1} . Elemental analysis calcd. for $\text{C}_{42}\text{H}_{66}\text{Li}_3\text{N}_3\text{O}_3\text{PSi}_3$: C 63.29, H 8.35, N 5.27; found: C 63.49, H 9.06, N 4.75.

$[\text{PN}_3]\text{Zr}(\text{NMe}_2)_2$ (2-Zr). A solution of $\text{Zr}(\text{NMe}_2)_4$ (120 mg, 451 μmol , 1.2 equiv) in toluene (10 mL) was added dropwise to a stirred solution of 1 (200 mg, 353 μmol , 1.0 equiv) in toluene (10 mL). The resulting yellow solution was heated to 130 $^\circ\text{C}$ for 5 days, and the dimethylamido byproduct was removed periodically by evacuating the headspace of the reaction vessel once per day. The solvent was then removed in vacuum, and the residue was washed with benzene (3 mL) and pentane (2 \times 5 mL). The product was obtained as a colorless solid (90 mg, 129 μmol , 33%). ^1H NMR (600 MHz, $\text{Tol}-d_8$): δ [ppm] =

7.06–7.03 (m, 6-ArH, 3 H), 7.02 (d, $^3J_{\text{H,H}} = 5.7$ Hz, 5-ArH, 3 H), 6.93 (d, $^3J_{\text{H,H}} = 7.4$ Hz, 3-ArH, 3 H), 6.83 (t, $^3J_{\text{H,H}} = 7.2$ Hz, 4-ArH, 3 H), 3.33 (s, NMe₂, 6 H), 2.71 (d, $^2J_{\text{H,P}} = 12.9$ Hz, PCH₂, 3 H), 2.28–2.11 (m, PCH₂, 3 H), –0.01 (s, SiMe₃, 27 H). ¹³C NMR (151 MHz, Tol-*d*₈): δ [ppm] = 150.5 (d, $^3J_{\text{C,P}} = 8.1$ Hz, 1-ArC), 131.9 (d, $^3J_{\text{C,P}} = 2.9$ Hz, 5-ArCH), 131.6 (s, 2-ArC), 130.9 (d, $^3J_{\text{C,P}} = 6.0$ Hz, 3-ArCH), 127.2 (s, 6-ArCH), 122.9 (s, 4-ArCH), 46.5 (s, NMe₂), 27.0 (d, $^1J_{\text{C,P}} = 4.4$ Hz, PCH₂), 2.8 (s, SiMe₃). ³¹P{¹H} NMR (243 MHz, Tol-*d*₈): δ [ppm] = 17.2 (s). MS (LIFDI): *m/z* (%) = 696.1 [M]⁺ (100%). M (C₃₂H₅₁N₄PSi₃Zr) = 698.23 g mol^{–1}. Elemental analysis calcd. for C₃₂H₅₁N₄PSi₃Zr: C 55.05, H 7.36, N 8.02; despite numerous attempts, low values for carbon were obtained, e.g., C 53.81, H 7.08, N 8.14.

[PN₃]Hf(NMe₂) (2-Hf). A solution of Hf(NMe₂)₄ (160 mg, 451 μ mol, 1.2 equiv) in toluene (10 mL) was added slowly to a stirred solution of **1** (200 mg, 353 μ mol, 1.0 equiv) in toluene (10 mL). An immediate color change to orange was observed, and the solution was heated to 130 °C for 18 days. Over this time, the dimethylamine byproduct was removed periodically by evacuating the headspace of the reaction vessel every third day. Subsequently, all volatiles were removed in vacuum and the residue was washed with benzene (5 mL) and pentane (5 mL). The product was obtained as a colorless solid (96 mg, 122 μ mol, 35%). ¹H NMR (600 MHz, Tol-*d*₈): δ [ppm] = 7.07–7.02 (m, 6-ArH, 3 H), 7.02 (d, $^3J_{\text{H,H}} = 10.4$ Hz, 5-ArH, 3 H), 6.90 (d, $^3J_{\text{H,H}} = 7.4$ Hz, 3-ArH, 3 H), 6.80 (t, $^3J_{\text{H,H}} = 7.0$ Hz, 4-ArH, 3 H), 3.40 (s, NMe₂, 6 H), 2.77 (dd, $^2J_{\text{H,P}} = 12.8$ Hz, $^3J_{\text{H,H}} = 2.6$ Hz, PCH₂, 3 H), 2.22 (t, $^2J_{\text{H,P}} = 12.7$ Hz, PCH₂, 3 H), –0.01 (s, SiMe₃, 27 H). ¹³C NMR (151 MHz, Tol-*d*₈): δ [ppm] = 150.0 (d, $^3J_{\text{C,P}} = 7.9$ Hz, 1-ArC), 132.7 (s, 5-ArCH), 131.7 (s, 2-ArC), 130.7 (d, $^3J_{\text{C,P}} = 5.7$ Hz, 3-ArCH), 127.2 (d, $^4J_{\text{C,P}} = 2.5$ Hz, 6-ArCH), 123.0 (s, 4-ArCH), 46.5 (s, NMe₂), 27.1 (d, $^1J_{\text{C,P}} = 4.4$ Hz, PCH₂), 2.9 (s, SiMe₃). ³¹P{¹H} NMR (243 MHz, Tol-*d*₈): δ [ppm] = 26.7 (s). MS (LIFDI): *m/z* (%) = 786.04 [M]⁺ (100%). M (C₃₃H₅₁N₄PSi₃Hf) = 785.49 g mol^{–1}. Elemental analysis calcd. for C₃₃H₅₁N₄PSi₃Hf: C 48.93, H 6.54, N 7.13; despite numerous attempts, low values for carbon were obtained, e.g., C 47.18, H 6.52, N 6.71.

[PN₃]ZrOTf (3-Zr). A solution of triethylsilyl trifluoromethanesulfonate (7.7 mg, 29 μ mol, 1.2 equiv) in toluene (5 mL) was slowly added to a solution of **2-Zr** (17 mg, 24 μ mol, 1.0 equiv) in toluene (5 mL) at –40 °C. The reaction mixture was allowed to warm to room temperature, and stirring at room temperature continued for 1 h. All volatiles were then removed in vacuum, and the residue was washed with a minimal amount of pentane and TMS₂O. The product was obtained as a white powder (10 mg, 12 μ mol, 51%). ¹H NMR (600 MHz, Tol-*d*₈): δ [ppm] = 7.09–7.08 (m, 6-ArH, 3 H), 7.00–6.94 (m, 5-ArH, 3 H), 6.87 (d, $^3J_{\text{H,H}} = 7.1$ Hz, 3-ArH, 3 H), 6.79 (t, $^3J_{\text{H,H}} = 7.6$ Hz, 4-ArH, 3 H), 2.64 (m, PCH₂, 3 H), 2.14–2.03 (m, PCH₂, 3 H), 0.03 (s, SiMe₃, 27 H). ¹³C NMR (151 MHz, Tol-*d*₈): δ [ppm] = 148.6 (d, $^3J_{\text{C,P}} = 8.0$ Hz, 1-ArC), 137.3 (s, 2-ArC), 130.9 (d, $^3J_{\text{C,P}} = 5.5$ Hz, 3-ArCH), 130.6 (d, $^5J_{\text{C,P}} = 2.6$ Hz, 5-ArCH), 129.5 (d, $^4J_{\text{C,P}} = 2.1$ Hz, 6-ArCH), 124.0 (s, 4-ArCH), 26.8 (d, $^1J_{\text{C,P}} = 10.6$ Hz, PCH₂), 1.65 (s, SiMe₃). ³¹P{¹H} NMR (243 MHz, Tol-*d*₈): δ [ppm] = 26.3 (s). M (C₃₁H₄₅F₃ZrN₃O₃PSSi₃) = 803.22 g mol^{–1}. Elemental analysis calcd. for C₃₁H₄₅F₃N₃O₃PSSi₃Zr: C 46.35, H 5.65, N 5.23; despite numerous attempts, low values for carbon were obtained, e.g., C 45.32, H 5.96, N 5.02.

[PN₃]HfOTf (3-Hf). A solution of triethylsilyl trifluoromethanesulfonate (10 mg, 38 μ mol, 1.2 equiv) in toluene (5 mL) was slowly added to a solution of **2-Hf** (25 mg, 32 μ mol, 1.0 equiv) in toluene (5 mL) at –40 °C. The reaction mixture was warmed to room temperature and stirred for 1 h. After removal of the solvent in vacuum, the residue was washed with a small amount of pentane and TMS₂O to afford the product as a white solid (16 mg, 18 μ mol, 47%). ¹H NMR (600 MHz, Tol-*d*₈): δ [ppm] = 7.09–7.08 (m, 6-ArH, 3 H), 7.08–7.07 (m, 5-ArH, 3 H), 6.87 (d, $^3J_{\text{H,H}} = 7.1$ Hz, 3-ArH, 3 H), 6.78 (t, $^3J_{\text{H,H}} = 6.5$ Hz, 4-ArH, 3 H), 2.75 (m, PCH₂, 3 H), 2.19 (t, $^2J_{\text{H,P}} = 14.0$ Hz, PCH₂, 3 H), 0.03 (s, SiMe₃, 27 H). ¹³C NMR (151 MHz, Tol-*d*₈): δ [ppm] = 148.0 (d, $^3J_{\text{C,P}} = 7.5$ Hz, 1-ArC), 131.8 (d, $^4J_{\text{C,P}} = 2.7$ Hz, 6-ArCH), 130.8 (d, $^3J_{\text{C,P}} = 5.8$ Hz, 3-ArCH), 130.1 (d, $^5J_{\text{C,P}} = 2.6$ Hz, 5-ArCH), 128.4 (s, 2-ArC), 124.1 (s, 4-ArCH), 26.9 (d, $^1J_{\text{C,P}} = 4.4$ Hz, PCH₂), 1.82 (s, SiMe₃). ³¹P{¹H} NMR (243 MHz, Tol-*d*₈): δ

[ppm] = 29.6 (s). MS (LIFDI): *m/z* (%) = 742.7 [M – OTf]⁺. M (C₃₁H₄₅F₃HfN₃O₃PSSi₃) = 890.49 g mol^{–1}. Elemental analysis calcd. for C₃₁H₄₅F₃HfN₃O₃PSSi₃: C 41.81, H 5.09, N 4.72; despite numerous attempts, low values for carbon were obtained, e.g., C 39.87, H 5.17, N 4.57.

[PN₃]TiCl (4-Ti). *Method A.* A suspension of **1-Li** (200 mg, 250 μ mol, 1.0 equiv) in toluene (5 mL) was added to a stirred suspension of TiCl₄(THF)₂ (91 mg, 270 μ mol, 1.1 equiv) in toluene (5 mL) at –40 °C. An immediate color change to deep red was observed, and the reaction mixture was allowed to warm to room temperature. Stirring at room temperature was continued for 6 h. The reaction mixture was then filtered through a plug of aluminum oxide. The orange-red filtrate was condensed to dryness, and the residual crude product was washed with a minimal amount of pentane. The product was obtained as a red solid after drying in vacuum for several hours (30 mg, 46 μ mol, 19%). ¹H NMR (600 MHz, Tol-*d*₈): δ [ppm] = 7.15 (d, $^3J_{\text{H,H}} = 8.1$ Hz, 6-ArH, 3 H), 7.01 (d, $^3J_{\text{H,H}} = 6.5$ Hz, 5-ArH, 3 H), 6.87 (d, $^3J_{\text{H,H}} = 7.4$ Hz, 3-ArH, 3 H), 6.79 (t, $^3J_{\text{H,H}} = 7.3$ Hz, 4-ArH, 3 H), 2.51 (dd, $J = 13.1$ Hz, 4.0 Hz, PCH₂, 3 H), 2.02 (dd, $J = 15.9$ Hz, 13.5 Hz, PCH₂, 3 H), 0.27 (s, SiMe₃, 27 H). ¹³C NMR (151 MHz, Tol-*d*₈): δ [ppm] = 154.4 (d, $^3J_{\text{C,P}} = 10.1$ Hz, 1-ArC), 130.1 (d, $^3J_{\text{C,P}} = 5.6$ Hz, 3-ArCH), 129.3 (s, 2-ArC), 127.3 (s, 6-ArCH), 127.2 (s, 5-ArCH), 123.7 (s, 4-ArCH), 26.9 (d, $^1J_{\text{C,P}} = 4.4$ Hz, PCH₂), 3.26 (s, SiMe₃). ³¹P{¹H} NMR (243 MHz, Tol-*d*₈): δ [ppm] = 40.7 (s). MS (LIFDI): *m/z* (%) = 645.1 [M]⁺ (100%). M (C₃₀H₄₅ClN₃PSi₃Ti) = 646.25 g mol^{–1}. Elemental analysis calcd. for C₃₀H₄₅ClN₃PSi₃Ti: C 55.76, H 7.02, N 6.50; found: C 55.38, H 6.38; N 6.18.

Method B. To a solution of **1** (60 mg, 106 μ mol, 1.0 equiv) in toluene (0.5 mL) was added Bn₃TiCl (38 mg, 106 μ mol, 1.0 equiv) at room temperature, resulting in an immediate color change to red. The resulting solution was heated to 55 °C for 4 h, and the solvent was removed in vacuum. The residue was extracted with a mixture of Et₂O and TMS₂O, and the extracts were kept at –40 °C for several days. Crystals of the intermediate [HNP₃]₂Ti(Bn)(Cl) formed over this time and were isolated by filtration (approximately 20 mg). ¹H NMR (600 MHz, Tol-*d*₈): δ [ppm] = 6.96 (d, $^3J_{\text{H,H}} = 8.1$ Hz, ArH, 2 H), 6.92 (m, ArH, 2 H), 6.84 (m, ArH, 4 H), 6.73 (m, ArH, 1 H), 6.69 (d, $^3J_{\text{H,H}} = 7.8$ Hz, 1 H), 6.58 (m, ArH, 1 H), 6.37 (d, $^3J_{\text{H,H}} = 7.4$ Hz, ArH, 1 H), 3.59 (m, PCH₂, 1 H), 3.17–3.10 (m, PCH₂, 1 H), 3.03 (s_{br}, Bn-CH₂, 2 H), 2.53–2.48 (m, PCH₂, 1 H), 2.41–2.40 (m, PCH₂, 1 H), 2.27 (d, $J = 13.1$ Hz, PCH₂, 1 H), 2.18 (m, PCH₂, 1 H), 0.53 (s, SiMe₃, 9 H), 0.22 (s, SiMe₃, 9 H), 0.13 (s, SiMe₃, 9 H). One crystal was selected for X-ray diffraction, and the remaining material was redissolved in toluene. The resulting solution (0.5 mL) was heated to 80 °C for 5 h and then condensed to dryness. No further work-up was required, and the product was obtained as a red solid (10 mg, 15 μ mol, 15%). Analytical data are identical with the data reported above (see method A).

[PN₃]ZrCl (4-Zr). *Method A.* A suspension of **1-Li** (400 mg, 495 μ mol, 1.0 equiv) in toluene (5 mL) was added to a stirred suspension of ZrCl₄(THF)₂ (190 mg, 504 μ mol, 1.0 equiv) in toluene (5 mL) at –40 °C, and the resulting reaction mixture was warmed to room temperature. The orange suspension was stirred at room temperature for 6 h and then filtered through Celite. The filtrate was condensed to dryness, and the residual yellowish material was washed with minimal amounts of pentane and TMS₂O. After drying in vacuum, a white powder of the product was obtained (149 mg, 231 μ mol, 47%). ¹H NMR (600 MHz, Tol-*d*₈): δ [ppm] = 7.10–7.09 (m, 6-ArH, 3 H), 7.03 (d, $^3J_{\text{H,H}} = 7.6$ Hz, 5-ArH, 3 H), 6.91 (d, $^3J_{\text{H,H}} = 7.4$ Hz, 3-ArH, 3 H), 6.80 (t, $^3J_{\text{H,H}} = 7.2$ Hz, 4-ArH, 3 H), 2.64 (dd, $^2J_{\text{H,P}} = 13.2$, $^3J_{\text{H,H}} = 3.3$ Hz, PCH₂, 3 H), 2.14–2.12 (m, PCH₂, 3 H), 0.15 (s, SiMe₃, 27 H). ¹³C NMR (151 MHz, Tol-*d*₈): δ [ppm] = 150.2 (d, $^3J_{\text{C,P}} = 8.4$ Hz, 1-ArC), 130.9 (d, $^3J_{\text{C,P}} = 5.3$ Hz, 3-ArCH), 130.0 (s, 2-ArC), 129.7 (s, 6-ArCH), 127.7 (s, 5-ArCH), 123.3 (s, 4-ArCH), 26.8 (d, $^1J_{\text{C,P}} = 4.4$ Hz, PCH₂), 2.3 (s, SiMe₃). ³¹P{¹H} NMR (243 MHz, Tol-*d*₈): δ [ppm] = 26.2 (s). MS (LIFDI): *m/z* (%) = 687.0 [M]⁺ (100%). M (C₃₀H₄₅ClN₃PSi₃Zr) = 689.61 g mol^{–1}. Elemental analysis calcd. for C₃₀H₄₅ClN₃PSi₃Zr: C 52.25, H 6.58, N 6.09; despite numerous attempts, low values for carbon were obtained, e.g., C 50.43, H 7.20, N 6.44.

Method B. A solution of trimethylsilyl chloride (43 μL , 353 μmol , 2.6 equiv) in toluene (1 mL) was slowly added to a solution of 2-Zr (90 mg, 129 μmol , 1.0 equiv) in toluene (5 mL), and the resulting mixture was stirred for 3 days at room temperature. All volatiles were removed in vacuum, and the residual material was washed with small amounts of pentane. The product is obtained as a white powder (35 mg, 54 μmol , 42%). Analytical data are identical with the data reported above (see method A).

[PN₂]HfCl (4-Hf). **Method A.** A suspension of 1-Li (100 mg, 125 μmol , 1.0 equiv) in toluene (5 mL) was added to a suspension of HfCl₄(THF)₂ (64 mg, 138 μmol , 1.1 equiv) in toluene (5 mL), at -40°C . After warming the reaction mixture to room temperature, stirring was continued 6 h. The resulting suspension was filtered through Celite, and the filtrate was condensed to dryness. The residual crude material was washed with minimal amounts of pentane and TMS₂O to afford the product as a pale yellow solid (54 mg, 70 μmol , 56%). ¹H NMR (600 MHz, Tol-*d*₈): δ [ppm] = 7.12 (d, ³J_{H,H} = 7.9 Hz, 6-ArH, 3 H), 7.03 (d, ³J_{H,H} = 6.5 Hz, 5-ArH, 3 H), 6.89 (d, ³J_{H,H} = 7.5 Hz, 3-ArH, 3 H), 6.78 (t, ³J_{H,H} = 7.3 Hz, 4-ArH, 3 H), 2.72 (dd, ²J_{H,P} = 13.1 Hz, ²J_{H,H} = 4.2 Hz, PCH₂, 3 H), 2.20 (m, PCH₂, 3 H), 0.15 (s, SiMe₃, 27 H). ¹³C NMR (151 MHz, Tol-*d*₈): δ [ppm] = 149.9 (d, ³J_{C,P} = 10.1 Hz, 1-ArC), 130.9 (d, ⁴J_{C,P} = 5.6 Hz, 6-ArCH), 130.7 (s, 2-ArC), 129.9 (s, 3-ArCH), 127.7 (s, 5-ArCH), 123.4 (s, 4-ArCH), 26.8 (d, ¹J_{C,P} = 4.4 Hz, PCH₂), 2.4 (s, SiMe₃). ³¹P{¹H} NMR (243 MHz, Tol-*d*₈): δ [ppm] = 31.7 (s). MS (LIFDI): *m/z* (%) = 776.94 [M]⁺ (100%). M (C₃₀H₄₅ClN₃PSi₃Hf) = 776.87 g mol⁻¹. Elemental analysis calcd. for C₃₀H₄₅ClHfN₃PSi₃: C 46.38, H 5.84, N 5.41; found: C 46.87, H 6.29, N 5.09.

Method B. A solution of trimethylsilyl chloride (8.2 μL , 65 μmol , 1.3 equiv) in toluene (0.2 mL) was slowly added to a solution of 2-Hf (35 mg, 50 μmol , 1.0 equiv) in toluene (0.3 mL). The resulting solution was kept at room temperature for 3 days, and all volatiles were then removed in vacuum. The residual material was washed with small amounts of pentane to afford the product as a colorless powder (18 mg, 23 μmol , 46%). Analytical data are identical with the data reported above (see method A).

[Me₂SiCH₂NPN₂]Ti (5-Ti). A precooled solution of Bn₂Mg(thf)₂ (50 mg, 137 μmol , 0.55 equiv) in toluene (4 mL) was slowly added to a solution of 4-Ti (160 mg, 250 μmol , 1.0 equiv) in toluene (5 mL) at -40°C . The resulting deep red reaction mixture was allowed to warm to room temperature, kept at this temperature for 1 h, and then heated to 90 $^\circ\text{C}$ for 9 h. After cooling the reaction mixture to room temperature, all volatiles were removed in vacuum and the residue was extracted with pentanes (25 mL). The pentane extracts were condensed to approximately 10 mL and left standing at -40°C overnight. The formed precipitate was filtered off and dried in vacuum to afford the product as an orange-red powder (100 mg, 164 μmol , 66%). ¹H NMR (600 MHz, C₆D₆): δ [ppm] = 7.14–7.11 (m, ArH, 2 H), 7.07–7.04 (m, ArH, 2 H), 6.93–6.87 (m, ArH, 2 H), 6.88–6.85 (m, ArH, 1 H), 6.84–6.80 (m, ArH, 2 H), 6.75–6.73 (m, ArH, 1 H), 2.69 (dd, ²J_{H,P} = 13.4, ²J_{H,H} = 4.1 Hz, PCH₂, 1 H), 2.59 (dd, ²J_{H,P} = 12.8, ²J_{H,H} = 5.8 Hz, PCH₂, 1 H), 2.50 (dd, ²J_{H,P} = 13.9, ²J_{H,H} = 5.4 Hz, PCH₂, 1 H), 2.38 (d, ²J_{H,H} = 11.7 Hz, TiCH₂, 1 H), 2.25 (m, PCH₂, 1 H), 2.05–1.91 (m, PCH₂, 2 H), 1.21 (d, ²J_{H,H} = 11.6 Hz, TiCH₂, 1 H), 0.77 (s, SiMe₂, 3 H), 0.21 (s, SiMe₃, 9 H), 0.19 (s, SiMe₃, 9 H), -0.00 (s, SiMe₂, 3 H). ¹³C NMR (101 MHz, C₆D₆): δ [ppm] = 155.3 (d, *J* = 11.6 Hz, ArC), 151.5 (d, *J* = 6.3 Hz, ArC), 150.6 (d, *J* = 11.3 Hz, ArC), 142.2 (s, ArC), 131.5 (d, *J* = 5.6 Hz, ArCH), 131.1 (d, *J* = 6.0 Hz, ArCH), 130.3 (d, *J* = 5.7 Hz, ArCH), 130.0 (s, ArC), 129.6 (d, *J* = 2.1 Hz, ArC), 129.0 (d, *J* = 3.2 Hz, ArCH), 128.5 (s, ArCH), 128.3 (d, *J* = 1.4 Hz, ArCH), 128.0 (d, *J* = 3.3 Hz, ArCH), 127.8 (d, *J* = 2.4 Hz, ArCH), 123.6 (s, ArCH), 123.1 (s, ArCH), 121.7 (d, *J* = 3.4 Hz, ArCH), 120.7 (s, ArCH), 28.1 (d, *J* = 4.6 Hz, PCH₂), 27.1 (d, ¹J_{C,P} = 11.9 Hz, PCH₂), 25.0 (d, ¹J_{C,P} = 9.1 Hz, PCH₂), 6.7 (s, TiCH₂), 6.6 (s, TiCH₂), 3.5 (s, SiMe₂), 2.6 (s, SiMe₃), 2.5 (s, SiMe₃). ³¹P{¹H} NMR (243 MHz, C₆D₆): δ [ppm] = 24.3 (s). M (C₃₁H₄₈N₃PSi₃Ti) = 625.83 g mol⁻¹. Elemental analysis calcd. for C₃₀H₄₄N₃PSi₃Ti: C 59.09, H 7.27, N 6.89; found: C 60.09, H 6.97, N 6.08.

■ ASSOCIATED CONTENT

📄 Supporting Information

Additional experimental details; selected NMR spectra; ORTEP plots of the molecular structures of 2-Hf, [HNP₂]-TiCl₂, [HNP₂]Ti(Bn)(Cl), and [(TMS)₂PN₂]₂Ti₃, crystallographic data, and details of the structure determinations for 1–4. This material is available free of charge via the Internet at <http://pubs.acs.org>.

■ AUTHOR INFORMATION

Corresponding Author

*E-mail: joachim.ballmann@uni-heidelberg.de. Tel: (+ 49) 6221-548596.

Notes

The authors declare no competing financial interest.

■ ACKNOWLEDGMENTS

Support for this research by a Liebig-Stipendium for J.B. and a FCI-Doktorandenstipendium for M.S. from the Fonds der Chemischen Industrie (FCI) is gratefully acknowledged. We thank Prof. L. Gade for generous support and continued interest in our work. We are grateful to Lukas Merz for experimental help with the synthesis of selected starting materials.

■ REFERENCES

- (1) Naini, A. A.; Menge, W. M. P. B.; Verkade, J. G. *Inorg. Chem.* **1991**, *30*, 5009–5012.
- (2) (a) Duan, Z.; Naini, A. A.; Lee, J.-H.; Verkade, J. G. *Inorg. Chem.* **1995**, *34*, 5477–5482. (b) Duan, Z.; Verkade, J. G. *Inorg. Chem.* **1995**, *34*, 4311–4316.
- (3) (a) Cummins, C. C.; Lee, J.; Schrock, R. R.; Davis, W. M. *Angew. Chem., Int. Ed.* **1992**, *31*, 1501–1503. (b) Cummins, C. C.; Schrock, R. R.; Davis, W. M. *Organometallics* **1992**, *11*, 1452–1454. (c) Schrock, R. R.; Cummins, C. C.; Wilhelm, T.; Lin, S.; Reid, S. M.; Kol, M.; Davis, W. M. *Organometallics* **1996**, *15*, 1470–1476.
- (4) Schubart, M.; O'Dwyer, L.; Gade, L. H.; Li, W.-S.; McPartlin, M. *Inorg. Chem.* **1994**, *33*, 3893–3898.
- (5) (a) Cummins, C. C.; Schrock, R. R. *Inorg. Chem.* **1994**, *33*, 395–396. (b) Duan, Z.; Verkade, J. G. *Inorg. Chem.* **1995**, *34*, 1576–1578. (c) Scott, P.; Hitchcock, P. B. *J. Chem. Soc., Chem. Commun.* **1995**, 579–580. (d) Freundlich, J. S.; Schrock, R. R. *Inorg. Chem.* **1996**, *35*, 7459–7461. (e) Neuner, B.; Schrock, R. R. *Organometallics* **1996**, *15*, 5–6. (f) Schrock, R. R. *Acc. Chem. Res.* **1997**, *30*, 9–16. (g) Roussel, P.; Alcock, N. W.; Scott, P. *Chem. Commun.* **1998**, 801–802. (h) Morton, C.; Munslow, I. J.; Sanders, C. J.; Alcock, N. W.; Scott, P. *Organometallics* **1999**, *18*, 4608–4613. (i) Chen, J.; Woo, L. K. *J. Organomet. Chem.* **2000**, *601*, 57–68. (j) Schrock, R. R.; Rosenberger, C.; Seidel, S. W.; Shih, K. Y.; Davis, W. M.; Odom, A. L. *J. Organomet. Chem.* **2001**, *617–618*, 495–501. (k) Filippou, A. C.; Schneider, S. *Organometallics* **2003**, *22*, 3010–3012. (l) Filippou, A. C.; Schneider, S.; Schnakenburg, G. *Angew. Chem., Int. Ed.* **2003**, *42*, 4486–4489. (m) Balazs, G.; Sierka, M.; Scheer, M. *Angew. Chem., Int. Ed.* **2005**, *44*, 4920–4924. (n) Leshinski, S.; Shalumova, T.; Tanski, J. M.; Waterman, R. *Dalton Trans.* **2010**, *39*, 9073–9078. (o) King, D. M.; Tuna, F.; McInnes, E. J. L.; McMaster, J.; Lewis, W.; Blake, A. J.; Liddle, S. T. *Science* **2012**, *337*, 717–720. (p) King, D. M.; Tuna, F.; McInnes, E. J. L.; McMaster, J.; Lewis, W.; Blake, A. J.; Liddle, S. T. *Nat. Chem.* **2013**, *5*, 482–488. (q) Tereniak, S. J.; Carlson, R. K.; Clouston, L. J.; Young, V. G., Jr.; Bill, E.; Maurice, R.; Chen, Y.-S.; Kim, H. J.; Gagliardi, L.; Lu, C. C. *J. Am. Chem. Soc.* **2014**, *136*, 1842–1855. (r) Gardner, B. M.; Cleaves, P. A.; Kefalidis, C. E.; Fang, J.; Maron, L.; Lewis, W.; Blake, A. J.; Liddle, S. T. *Chem. Sci.* **2014**, DOI: 10.1039/C4SC00182F. (s) Parsell, T. H.; Yang, M.-Y.; Borovik, A. S. *J. Am. Chem. Soc.* **2009**, *131*, 2762–2763. (t) England, J.

Farquhar, E. R.; Guo, Y.; Cranswick, M. A.; Ray, K.; Münck, E.; Que, L., Jr. *Inorg. Chem.* **2011**, *50*, 2885–2896.

(6) (a) Pinkas, J.; Gaul, B.; Verkade, J. G. *J. Am. Chem. Soc.* **1993**, *115*, 3925–3931. (b) Plass, W.; Verkade, J. G. *Inorg. Chem.* **1993**, *32*, 5153–5159. (c) Pinkas, J.; Wang, T.; Jacobson, R. A.; Verkade, J. G. *Inorg. Chem.* **1994**, *33*, 5244–5253. (d) Pinkas, J.; Wang, T.; Jacobson, R. A.; Verkade, J. G. *Inorg. Chem.* **1994**, *33*, 4202–4210. (e) Duan, Z.; Young, V. G., Jr.; Verkade, J. G. *Inorg. Chem.* **1995**, *34*, 2179–2185. (f) Plass, W.; Pinkas, J.; Verkade, J. G. *Inorg. Chem.* **1997**, *36*, 1973–1978. (g) Morton, C.; Alcock, N. W.; Lees, M. R.; Munslow, I. J.; Sanders, C. J.; Scott, P. J. *Am. Chem. Soc.* **1999**, *121*, 11255–11256. (h) Shutov, P. L.; Karlov, S. S.; Harms, K.; Tyurin, D. A.; Churakov, A. V.; Lorberth, J.; Zaitseva, G. S. *Inorg. Chem.* **2002**, *41*, 6147–6152. (i) Shutov, P. L.; Sorokin, D. A.; Karlov, S. S.; Harms, K.; Oprunenko, Y. F.; Churakov, A. V.; Antipin, M. Y.; Zaitseva, G. S.; Lorberth, J. *Organometallics* **2003**, *22*, 516–522. (j) Shutov, P. L.; Karlov, S. S.; Harms, K.; Churakov, A. V.; Lorberth, J.; Zaitseva, G. S. *Eur. J. Inorg. Chem.* **2004**, 2123–2129. (k) Verkade, J. G. *Acc. Chem. Res.* **1993**, *26*, 483–489.

(7) (a) Yandulov, D. V.; Schrock, R. R. *Science* **2003**, *301*, 76–78. (b) Reithofer, M. R.; Schrock, R. R.; Müller, P. J. *Am. Chem. Soc.* **2010**, *132*, 8349–8358. (c) Kinney, R. A.; McNaughton, R. L.; Chin, J. M.; Schrock, R. R.; Hoffman, B. M. *Inorg. Chem.* **2011**, *50*, 418–420. (d) Cain, M. F.; Forrest, W. P., Jr.; Peryshkov, D. V.; Schrock, R. R.; Müller, P. J. *Am. Chem. Soc.* **2013**, *135*, 15338–15341. (e) MacBeth, C. E.; Golombek, A. P.; Young, V. P., Jr.; Yang, C.; Kuczera, K.; Hendrich, M. P.; Borovik, A. S. *Science* **2000**, *289*, 938–941.

(8) (a) Waterman, R. *Chem. Soc. Rev.* **2013**, *42*, 5629–5641. (b) Waterman, R. *Curr. Org. Chem.* **2012**, *16*, 1313–1331. (c) Ghebreab, M. B.; Newsham, D. K.; Waterman, R. *Dalton Trans.* **2011**, *40*, 7683–7685.

(9) Schwarz, A. D.; Herbert, K. R.; Paniagua, C.; Mountford, P. *Organometallics* **2010**, *29*, 4171–4188.

(10) (a) Lensink, C.; Xi, S. K.; Daniels, L. M.; Verkade, J. G. *J. Am. Chem. Soc.* **1989**, *111*, 3478–3479. (b) Arumugam, S.; Verkade, J. G. *J. Org. Chem.* **1997**, *62*, 4827–4828. (c) Kisanga, P. B.; Verkade, J. G.; Schwesinger, R. *J. Org. Chem.* **2000**, *65*, 5431–5432. (d) Chintareddy, V. R.; Wadhwa, K.; Verkade, J. G. *J. Org. Chem.* **2009**, *74*, 8118–8132. (e) Wadhwa, K.; Chintareddy, V. R.; Verkade, J. G. *J. Org. Chem.* **2009**, *74*, 6681–6690. (f) Wadhwa, K.; Verkade, J. G. *J. Org. Chem.* **2009**, *74*, 5683–5686. (g) Chintareddy, V. R.; Ellern, A.; Verkade, J. G. *J. Org. Chem.* **2010**, *75*, 7166–7174. (h) Raytchev, P. D.; Martinez, A.; Gornitzka, H.; Dutasta, J.-P. *J. Am. Chem. Soc.* **2011**, *133*, 2157–2159. (i) Chatelet, B.; Joucla, L.; Dutasta, J.-P.; Martinez, A.; Szeto, K. C.; Dufaud, V. *J. Am. Chem. Soc.* **2013**, *135*, 5348–5351.

(11) (a) Blackman, A. G. *Polyhedron* **2005**, *24*, 1–39. (b) Çelenligil-Çetin, R.; Paraskevopoulou, P.; Dinda, R.; Staples, R. J.; Sinn, E.; Rath, N. P.; Stavropoulos, P. *Inorg. Chem.* **2008**, *47*, 1165–1172. (c) Paraskevopoulou, P.; Ai, L.; Wang, Q.; Pinnareddy, D.; Acharyya, R.; Dinda, R.; Das, P.; Çelenligil-Çetin, R.; Floros, G.; Sanakis, Y.; Choudhury, A.; Rath, N. P.; Stavropoulos, P. *Inorg. Chem.* **2010**, *49*, 108–122.

(12) (a) Groysman, S.; Segal, S.; Goldberg, I.; Kol, M.; Goldschmidt, Z. *Inorg. Chem. Commun.* **2004**, *7*, 938–941. (b) Lehtonen, A.; Sillanpää, R. *Organometallics* **2005**, *24*, 2795–2800. (c) Licini, G.; Mba, M.; Zonta, C. *Dalton Trans.* **2009**, 5265–5277.

(13) (a) Govindaswamy, N.; Quarless, D. A., Jr.; Koch, S. A. *J. Am. Chem. Soc.* **1995**, *117*, 8468–8469. (b) Motekaitis, R. J.; Martell, A. E.; Koch, S. A.; Hwang, J.; Quarless, D. A., Jr.; Welch, M. J. *Inorg. Chem.* **1998**, *37*, 5902–5911.

(14) (a) Block, E.; Ofori-Oakai, G.; Zubieta, J. *J. Am. Chem. Soc.* **1989**, *111*, 2327–2329. (b) Chu, W.-C.; Wu, C.-C.; Hsu, H.-F. *Inorg. Chem.* **2006**, *45*, 3164–3166. (c) Conradie, J.; Quarless, D. A., Jr.; Hsu, H.-F.; Harrop, T. C.; Lippard, S. J.; Koch, S. A.; Ghosh, A. *J. Am. Chem. Soc.* **2007**, *129*, 10446–10456. (d) Lee, C.-M.; Chen, C.-H.; Liao, F.-X.; Hu, C.-H.; Lee, G.-H. *J. Am. Chem. Soc.* **2010**, *132*, 9256–9258. (e) Ye, S.; Neese, F.; Ozarowski, A.; Smirnov, D.; Krzystek, J.; Telsler, J.; Liao, J.-H.; Hung, C.-H.; Chu, W.-C.; Tsai, Y.-F.; Wang, R.-C.; Chen, K.-Y.; Hsu, H.-F. *Inorg. Chem.* **2010**, *49*, 977–988. (f) Chang, Y.-H.; Su, C.-

L.; Wu, R.-R.; Liao, J.-H.; Liu, Y.-H.; Hsu, H.-F. *J. Am. Chem. Soc.* **2011**, *133*, 5708–5711. (g) Lee, C.-M.; Chuo, C.-H.; Chen, C.-H.; Hu, C.-C.; Chiang, M.-H.; Tseng, Y.-J.; Hu, C.-H.; Lee, G.-H. *Angew. Chem., Int. Ed.* **2012**, *51*, 5427–5430.

(15) (a) Han, H.; Elsmaili, M.; Johnson, S. A. *Inorg. Chem.* **2006**, *45*, 7435–7445. (b) Han, H.; Johnson, S. A. *Organometallics* **2006**, *25*, 5594–5602. (c) Hatnean, J. A.; Raturi, R.; Lefebvre, J.; Leznoff, D. B.; Lawes, G.; Johnson, S. A. *J. Am. Chem. Soc.* **2006**, *128*, 14992–14999. (d) Keen, A. L.; Doster, M.; Han, H.; Johnson, S. A. *Chem. Commun.* **2006**, 1221–1223. (e) Han, H.; Johnson, S. A. *Eur. J. Inorg. Chem.* **2008**, 471–482. (f) Raturi, R.; Lefebvre, J.; Leznoff, D. B.; McGarvey, B. R.; Johnson, S. A. *Chem.—Eur. J.* **2008**, *14*, 721–730.

(16) (a) Hölscher, M.; Leitner, W. *Eur. J. Inorg. Chem.* **2006**, 4407–4417. (b) Schenk, S.; Reiher, M. *Inorg. Chem.* **2009**, *48*, 1638–1648.

(17) (a) Smythe, N. C. Ph.D. Dissertation, Massachusetts Institute of Technology, Cambridge, MA, 2006 (available via the Internet at <http://hdl.handle.net/1721.1/37838>). (b) Fryzuk, M. D. Personal communication. (c) Hounjet, L. J.; Bierenstiel, M.; Ferguson, M. J.; McDonald, R.; Cowie, M. *Dalton Trans.* **2009**, 4213–4226.

(18) (a) Sietzen, M.; Wadepohl, H.; Ballmann, J. *Organometallics* **2014**, *33*, 612–615. (b) Sietzen, M.; Wadepohl, H.; Ballmann, J. Unpublished results.

(19) (a) Chen, H. G.; Hoehstetter, C.; Knochel, P. *Tetrahedron Lett.* **1989**, *30*, 4795–4798. (b) Andrés, J. I.; Alonso, J. M.; Fernández, J.; Iturrino, L.; Martínez, P.; Meert, T. F.; Sipido, V. K. *Bioorg. Med. Chem. Lett.* **2002**, *12*, 3573–3577. (c) Schroer, J.; Wagner, S.; Abram, U. *Inorg. Chem.* **2010**, *49*, 10694–10701.

(20) Issleib, K.; Winkelmann, H.; Abicht, H. P. *Synth. React. Inorg. Met.-Org. Chem.* **1974**, *4*, 191–203.

(21) Upadhyay, S. K.; Jursic, B. S. *Synth. Commun.* **2011**, *41*, 3177–3185.

(22) (a) Albers, H.; Schuler, W. *Ber. Dtsch. Chem. Ges.* **1943**, *76B*, 23–26. (b) Jacobs, H.; Hassiepen, K. M. *Z. Anorg. Allg. Chem.* **1985**, *531*, 108–118.

(23) Schäfer, H.; Fritz, G.; Hölderich, W. Z. *Anorg. Allg. Chem.* **1977**, *428*, 222–224.

(24) Easton, C. J.; Hutton, C. A. *Synlett* **1998**, 457–466.

(25) Landaeta, V. R.; Peruzzini, M.; Herrera, V.; Bianchini, C.; Sanchez-Delgado, R. A.; Goeta, A. E.; Zanolini, F. *J. Organomet. Chem.* **2006**, *691*, 1039–1050.

(26) (a) MacLachlan, E. A.; Hess, F. M.; Patrick, B. O.; Fryzuk, M. D. *J. Am. Chem. Soc.* **2007**, *129*, 10895–10905. (b) Morello, L.; Joao Ferreira, M.; Patrick, B. O.; Fryzuk, M. D. *Inorg. Chem.* **2008**, *47*, 1319–1323. (c) Menard, G.; Jong, H.; Fryzuk, M. D. *Organometallics* **2009**, *28*, 5253–5260. (d) Zhu, T.; Wambach, T. C.; Fryzuk, M. D. *Inorg. Chem.* **2011**, *50*, 11212–11221.

(27) Wang, C.; Erker, G.; Kehr, G.; Wedeking, K.; Fröhlich, R. *Organometallics* **2005**, *24*, 4760–4773.

(28) Benzeng, E.; Kornicker, W. *Chem. Ber.* **1961**, *94*, 2263–2267.

(29) Zucchini, U.; Albizzati, E.; Giannini, U. *J. Organomet. Chem.* **1971**, *26*, 357–372.

(30) Manzer, L. E. *Inorg. Synth.* **1982**, *21*, 135–140.

(31) Reich, H. J. *Chem. Rev.* **2013**, *113*, 7130–7178.

(32) Bailey, P. J.; Coxall, R. A.; Dick, C. M.; Fabre, S.; Henderson, L. C.; Herber, C.; Liddle, S. T.; Loroño-Gonzalez, D.; Parkin, A.; Parsons, S. *Chem.—Eur. J.* **2003**, *9*, 4820–4828.

(33) Waterman, R. *Organometallics* **2007**, *26*, 2492–2494.

(34) Roering, A. J.; Maddox, A. F.; Elrod, L. T.; Chan, S. M.; Ghebreab, M. B.; Donovan, K. L.; Davidson, J. J.; Hughes, R. P.; Shalumova, T.; MacMillan, S. N.; Tanski, J. M.; Waterman, R. *Organometallics* **2009**, *28*, 573–581.